

Lattice-gas model for alkali-metal fullerenes: face-centered-cubic structure

László Udvardi

*Quantum Theory Group, Institute of Physics, Technical University of Budapest,
H-1111 Budapest, Budafoki út 8, Hungary*

György Szabó

Research Institute for Materials Science, H-1525 Budapest, POB 49, Hungary

A lattice-gas model is suggested for describing the ordering phenomena in alkali-metal fullerenes of face-centered-cubic structure assuming that the electric charge of alkali ions residing in either octahedral or tetrahedral sites is completely screened by the first-neighbor C_{60} molecules. This approximation allows us to derive an effective ion-ion interaction. The van der Waals interaction between the ion and C_{60} molecule is characterized by introducing an additional site energy at the tetrahedral sites. This model is investigated by using a three-sublattice mean-field approximation and a simple cluster-variation method. The analysis shows a large variety of phase diagrams when changing the site energy parameter.

64.60.Cn, 05.70.-a, 61.43.Bn

(August 15, 2018)

I. INTRODUCTION

Since the discovery of superconductivity in several alkali-metal fullerenes [1–3] a large variety of A_xC_{60} intercalation compounds has been prepared and investigated (for recent reviews see papers [4,5]). In the face-centered-cubic (FCC) structure of pristine C_{60} the molecules are bonded via van der Waals interaction. In this structure the tetrahedral and octahedral interstitial spaces are sufficiently large to accommodate alkali atoms without significant distortion of the lattice. The intercalated alkali atoms transfer their s electron to C_{60} molecules, consequently, the lattice is contracted by the electrostatic interaction for small atoms (e.g. Na).

Because of the charge transfer the electrostatic energy plays an important role in the formation of different ordered structures, as well as in the distortion of the host lattice for large alkali concentration ($x > 3$). Fleming *et al.* [6] have determined the electrostatic energies for Rb_xC_{60} compounds assuming point charges for the Rb^+ ions, and the contribution of the C_{60}^{x-} ion is expressed as the minimum Coulomb repulsion of x point charges on a sphere of radius R , with R taken to be the C_{60} nucleon radius of 3.5 Å. In the calculation of electrostatic energies Rabe *et al.* [7] have assumed a uniformly charged spherical shell with the same radius for the C_{60}^{x-} ion.

In the present work we introduce a simple lattice-gas model to study the ordering phenomena in alkali fullerenes. In this model the interstitial sites may be empty or occupied by one type of alkali ion. In agreement with the large size of fullerenes, here we assume that an A^+ alkali ion is completely screened by uniformly distributing its transferred charge on the first neighbor C_{60} molecules. For example, the alkali ion residing at a tetrahedral (octahedral) site is surrounded by four (six) C_{60} molecules with charges of $-e/4$ ($-e/6$). In other words, each inter-

calated alkali atom transfers charges to its neighboring C_{60} molecules independently of the position of the remaining A^+ . This simplification makes the derivation of an effective pair interaction possible, which is evidently a short range one. The difference between the sizes of tetrahedral and octahedral voids is considered by introducing extra site energy related to the van der Waals interactions. This site energy parameter depends on the radius of the intercalated particle, consequently it is characteristic of the type of alkali atom. In the knowledge of the effective interactions (and site energy) characterized by a few parameters we are able to study the ordering within the framework of the lattice-gas (Ising) formalism. Accepting the spherical shell charge distribution on C_{60} as suggested by Rabe *et al.* [7] this model reproduces the ordered ground state energies given by them. A simple mean-field analysis is carried out to demonstrate the richness of phase diagrams when varying two parameters (site energy and radius of the spherical shell).

The above formalism can describe the ordered structures observed in alkali fullerenes with FCC structure. Namely, in pristine C_{60} all the interstitial sites are empty, whereas in the superconducting compounds with nominal composition A_3C_{60} both the octahedral and tetrahedral sites are occupied by alkali ions. [8,1–3] Only the octahedral sites are occupied in AC_{60} forming NaCl structure for $A=Rb$ and Cs . [9] Filling of the tetrahedral sites results in the CaF_2 structure observed by Rossiensky *et al.* [10] in the Na_xC_{60} system. According to our analysis the above phases are found to be stable if one takes the total energy of charged C_{60} molecule into consideration as discussed later on.

The early experimental investigations of the alkali intercalated fullerenes are summarized by Zhu *et al.* [11] in a provisional phase diagram. Recently, Poirier and Weaver [12] and Kuzmany *et al.* [13] proposed a phase diagram

for the K_xC_{60} system showing a eutectoid transformation from the homogeneous KC_{60} state to the composition of C_{60} and K_3C_{60} phases. [12] Our calculation confirms the existence of such a phase digram in a narrow range of parameters.

The above model explains adequately the formation of different intercalated structures. Our purpose is not to argue that the present description gives the correct lattice-gas model for a given A_xC_{60} system but rather to emphasize some general features highlighted by this approach because the model is adaptable for other metal- C_{60} systems. By this means the present model provides a framework to classify these systems. The relevant features will be illuminated by displaying a set of distinct phase diagrams.

In this paper we restrict ourselves to the systems corresponding to A_xC_{60} with rigid FCC structure. The present description consider the C_{60} molecule as a spherical object, that is, the phenomena related to the orientational ordering are neglected. Both the interaction between two C_{60} molecules and the electronic structure are simplified therefore the present model can not describe the chain formation discovered very recently by Chauvet *et al.* [14]

The lattice-gas model is derived in the subsequent section. In Sec. III we discuss the ground states suggested by the model for different values of site energy. A three-sublattice mean-field analysis is performed in Sec. IV to demonstrate the variety of phase diagrams. These results are confirmed by a simple (triangular) version of the cluster-variation method (CVM) in Sec. V. Finally we summarize our conclusions and discuss the possible continuation of the present approach in Sec. VI.

II. THE MODEL

The electronic structure calculations for alkali fullerenes have indicated that the higher lying s bands of the metal are unoccupied and the electrons fill the empty t_{1u} states of the C_{60} molecule, so the alkali atoms are ionized and their valence electrons are accepted by the fullerene molecule forming a negative ion. [15,16] In such a situation the Coulomb interaction has the most important contribution to the energy of the system. Several authors have already studied the effect of the Madelung energy on the charge-transfer solids [17], binary [18,19] and pseudobinary alloys [20] and intercalated graphite compounds [21].

Statistical physics is able to give an adequate description of the Ising systems with short range interaction but a great deal arises in handling the infinite range Coulomb interaction. An effective way of eliminating this problem is to construct a renormalized short range interaction. For this purpose one can, for example, use the cluster expansion of the Madelung energy. [19] In our treatment a well converging series of pair interactions is derived in

order to avoid the difficulties arising from the long range order interactions among the ions.

Calculations taking into account the polarizability of the fullerene molecules in the host lattice [22] suggested that the energy of two charged C_{60} molecules in the intercalated solid can be well described as the interaction between two point charges in a dielectric media characterized by ε .

According to that when calculating the Coulomb energy of the system, the metal atoms and C_{60} molecules are treated as point charges. The charge of the alkali atoms has been taken to be e and the charge of the C_{60} has been strongly related to the occupation of the nearest neighbor interstitial sites. The charge distribution may easily be described in the lattice-gas formalism introducing the site occupation variables η_i which is 1 if the i -th interstitial site is occupied and 0 if this site is empty. Within this formalism the charge at site i is evidently $q_i = e\eta_i$ and the charge transferred to the α -th C_{60} molecule can be written as:

$$Q_\alpha = -e \sum_{j \in N_\alpha} c_j \eta_j \quad (1)$$

where N_α means the set of first neighbor tetrahedral and octahedral interstitial sites around the α -th C_{60} molecule and c_j denotes the portion of charge transferred from the alkali atom residing at the j -th site to each nearest neighbor C_{60} molecule. More precisely, $c_j = 1/6$ for octahedral and $1/4$ for tetrahedral sites. Such a choice provides that each alkali ion is completely neutralized by its first neighbor C_{60} molecules. The model assumes that the transferred charges accompanies the alkali ions when hopping from site to site. This charge distribution evidently satisfies the requirement of the neutrality of the crystal.

The energy of the system can be given in the following form:

$$E = \frac{1}{2\varepsilon} \sum_{i \neq j} \frac{q_i q_j}{r_{ij}} + \frac{1}{2\varepsilon} \sum_{\alpha \neq \beta} \frac{Q_\alpha Q_\beta}{r_{\alpha\beta}} + \sum_{i, \alpha} \frac{q_i Q_\alpha}{\varepsilon r_{i\alpha}} + \sum_{\alpha} E_{int}(Q_\alpha) \quad (2)$$

where $E_{int}(Q_\alpha)$ is the intramolecular energy, the Greek and Latin indices run over the C_{60} sites and interstitial sites of the FCC lattice respectively. Substituting the charges from (1) the Coulomb energy can be expressed as:

$$E_C = \frac{e^2}{2\varepsilon} \sum_{i \neq j} \frac{1}{r_{ij}} \eta_i \eta_j - \frac{e^2}{\varepsilon} \sum_{i, \alpha} \sum_{j \in N_\alpha} \frac{c_j}{r_{i\alpha}} \eta_i \eta_j + \frac{e^2}{2\varepsilon} \sum_{\alpha \neq \beta} \sum_{j \in N_\alpha} \sum_{k \in N_\beta} \frac{c_j c_k}{r_{\alpha\beta}} \eta_j \eta_k. \quad (3)$$

On exchanging the order of summations the energy can be separated into the contributions of onsite and pair interactions, namely

$$E_C = \sum_i \epsilon'_i \eta_i + \frac{1}{2} \sum_{ij} V'_{ij} \eta_i \eta_j \quad (4)$$

where

$$\epsilon'_i = \frac{e^2}{2\epsilon} \sum_{(\alpha,\beta) \in N_i, \alpha \neq \beta} \frac{c_i^2}{r_{\alpha\beta}} - \frac{e^2}{\epsilon} \sum_{\alpha \in N_i} \frac{c_j}{r_{i\alpha}}, \quad (5)$$

$$V'_{ij} = \frac{e^2}{\epsilon r_{ij}} + \frac{e^2}{\epsilon} \sum_{\alpha \in N_i} \sum_{\beta \in N_j} c_i c_j \frac{(1 - \delta_{\alpha\beta})}{r_{\alpha\beta}} - \frac{e^2}{\epsilon} \sum_{\alpha \in N_j} \frac{c_j}{r_{i\alpha}} - \frac{e^2}{\epsilon} \sum_{\alpha \in N_i} \frac{c_i}{r_{j\alpha}}, \quad (6)$$

and N_i denotes the set of first neighbor C_{60} positions around interstitial site i .

The magnitude of V'_{ij} decreases rapidly with the distance between sites i and j . One can realize in Eq. 6 the Coulomb interaction between two cluster formed by the i -th and j -th alkali ion as the central site and their nearest neighbor C_{60} molecules. Since the clusters are neutral and the systems have cubic symmetry the monopole, dipole and the quadrupole terms vanish. So there are only higher order multipole interactions between two sites. The good convergence properties of the pair interaction is a consequence of our basic assumptions, viz. the nearest neighbor shell of the C_{60} molecules completely screens out the alkali ion charge.

In order to evaluate the intramolecular energy a series of UHF-MNDO [23] calculations have been performed for up to a sixfold ionized single C_{60}^{x-} molecule where the characteristic bond lengths of the system were kept constant $r_1 = 1.400 \text{ \AA}$ and $r_2 = 1.440 \text{ \AA}$.

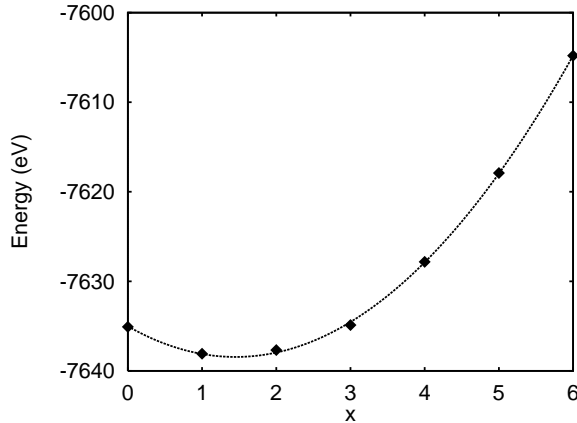


FIG. 1. Total energy of C_{60}^{x-} ion. Diamonds are the calculated values, dashed line represents the fitted parabola.

The total energy of the charged molecule as a function of the number of excess electrons can be fitted quite well with a parabola (see Fig. 1) given by:

$$E_{tot} = A + Bx + Cx^2 \quad (7)$$

where x is the number of extra electrons on the molecule and $A = -7635.02 \text{ eV}$; $B = -4.71926 \text{ eV}$; $C = 1.6262 \text{ eV}$.

Such an almost perfect parabolic behavior does not hold for other fullerenes with lower symmetry.

The quadratic energy dependence of the isolated molecule on the excess charges allows us to introduce an effective radius for the C_{60} molecule having a value of $R = 0.312a$ where the lattice constant a is given by experiment [8]. From previous calculations [22,24,25] $R \approx 4.8 \text{ \AA}$ can be obtained. The differences between the present and the cited calculations are due to the different choice of the equilibrium bond lengths. Since the C_{60} molecule is embedded in the crystal lattice the energy of the single molecule is modified by the surrounding media. Supposing dielectric screening mechanism one can apply the Onsager-Kirkwood theory of the electrostatic solvation [26] for estimating the effect of the lattice:

$$E_{int} = E_0 - \frac{1}{2} \left(\left(1 - \frac{1}{\epsilon}\right) \frac{Q^2}{r_0} + 2 \frac{\epsilon - 1}{2\epsilon + 1} \frac{\mu^2}{r_0^3} + \dots \right) \quad (8)$$

where r_0 is the radius of the cavity into which the molecule is embedded. Since the μ dipole moment of the charged C_{60} is zero choosing the radius of the cavity to be equal the effective radius the intramolecular energy can be written as:

$$E_{int} = A + Bx + \frac{e^2 x^2}{2\epsilon R} \quad (9)$$

The first term gives a constant contribution to the total energy and the linear term shifts the onsite energies. Both effects may be transformed out by rescaling energy. The spherical shell model proposed by Rabe *et al.* [7] with the original radius of the bucky-ball leads essentially different ordering properties. The quadratic term gives a V''_{ij} contribution to the pair interaction between those alkali ions which transfer some charge to the same C_{60} molecule, i.e.:

$$V''_{ij} = \frac{2}{\epsilon} \sum_{\alpha} c_i c_j C \quad (10)$$

where $\alpha \in N_i \cap N_j$. Obviously, this contribution vanishes when r_{ij} exceeds a threshold value. Furthermore, the energy of C_{60}^{x-} increases the site energies too with

$$\epsilon''_i = \frac{1}{\epsilon} \sum_{\alpha \in N_i} c_i^2 C. \quad (11)$$

The contribution of the van der Waals interaction to the site energy is distinct for the tetrahedral and octahedral sites and depends on the size of the alkali ion. To characterize this contribution we introduce an additional site energy, i.e.:

$$\epsilon_i = \begin{cases} \epsilon_o & \text{for octahedral sites,} \\ \epsilon_t + \delta E_t & \text{for tetrahedral sites} \end{cases} \quad (12)$$

where δE_t is considered as the difference between the two types of sites and is expected to be positive for large

alkali ions. In this expression the sum of ϵ'_i and ϵ''_i is indicated by ϵ_o and ϵ_t for the octahedral and tetrahedral sites, respectively. The numerical calculations give $\epsilon_o = -1.17817e^2/\epsilon a$ and $\epsilon_t = -1.37843e^2/\epsilon a$ (where $e^2/a \approx 1$ eV), i.e. the tetrahedral sites are primarily occupied for $\delta E_t = 0$.

We are now in a position to express the total energy of the system within the lattice-gas formalism. The following Hamiltonian defines the energy for any configuration of alkali ions described by the variables η_i :

$$H = \sum_i \epsilon_i \eta_i + \frac{1}{2} \sum_{ij} V_{ij} \eta_i \eta_j, \quad (13)$$

where $V_{ij} = V'_{ij} + V''_{ij}$ and ϵ_i , V'_{ij} , V''_{ij} are defined above by Eqs. (12), (6) and (10).

The effective pair interactions V_{ij} vs. r_{ij}/a are shown in Fig. 2. V_{ij} has different values for the same distances; in other words, the pair interaction depends on the orientation of the pair for some values of r_{ij} . Figure 2 demonstrates clearly that V_{ij} becomes extremely weak if $r_{ij} > a$. The attractive contributions of the effective pair interaction (for $a/2 < r_{ij} \leq a$) indicates the stability of alkali intercalated fullerides at large alkali concentrations.

As a comparison V'_{ij} is also plotted in Fig. 2. The striking difference between V_{ij} and V'_{ij} indicates the important role of the electronic energy of C_{60}^{x-} ions as will be investigated in detail in the subsequent sections.

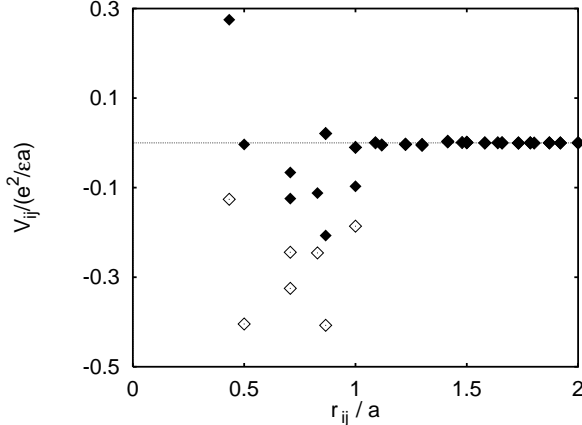


FIG. 2. Effective pair interaction as a function of ion-ion distance. Open diamonds represent the pure coulombic interaction (V'_{ij}), closed diamonds refer to full interaction (V_{ij}) including the energy of charged C_{60} molecule.

III. GROUND STATES

The electrostatic energies of some ordered structures have already been investigated. [6,7] Now we concentrate on analysing such FCC structures which may be described by introducing three sublattices as demonstrated in Fig. 3. The sites of each sublattice form a FCC structure equivalent to the cage lattice. For later convenience

the sublattices are labelled 0 for octahedral and 1 or 2 for tetrahedral sites. In the three-sublattice formalism the states are characterized by a vector consisting of sublattice occupations. For example, the state $(\sigma_0, \sigma_1, \sigma_2)$ denotes an alkali distribution where the sites of sublattice ν are occupied with a probability σ_ν . In general $0 \leq \sigma_\nu \leq 1$, however, $\sigma_\nu = 0$ or 1 for ordered structures. These ordered states are well known in crystallography. For example, the states $(1,0,0)$, $(0,1,1)$ and $(1,1,1)$ are equivalent to the NaCl, CaF_2 , and BiF_3 structures.

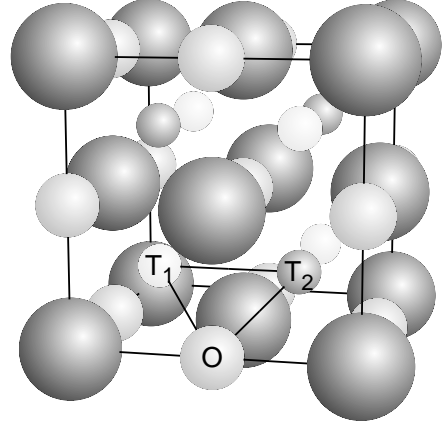


FIG. 3. Arrangement of octahedral (medium size spheres) and the two tetrahedral (dark and light small spheres) interstitial sites in an FCC lattice formed by C_{60} molecules (large spheres). The triangle represents the basic cluster of our CVM approximation.

One can easily see that according to the present model the C_{60} molecules are uniformly charged for the ordered states defined above. Consequently, the electrostatic energies are equivalent to the Madelung energies determined previously. [6,7] In agreement with the expectation the energies of ordered states are equivalent to those predicted by Rabe *et al.* [7] when choosing $R = 3.5 \text{ \AA}$. In the above model, however, we have chosen larger R as detailed in the previous section. This correction modifies the total energy of the ordered states as plotted in Fig. 4 for $\delta E_t = 1.1$. As a result the present model suggests three stable ground states $[(0,0,0)$, $(1,0,0)$ and $(1,1,1)]$, which are connected by solid lines in the figure. That is, the system with a nominal alkali content $x = 1$ has $(1,0,0)$ phase in contrast to the former model predicting a stable $(0,1,0)$ phase. [7]

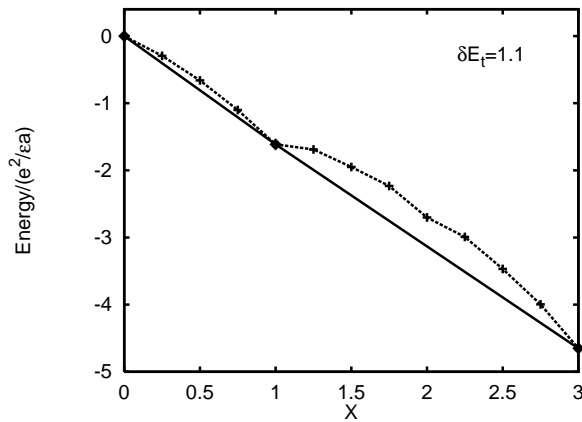


FIG. 4. Smallest electrostatic energies of the different ordered structures of A_xC_{60} at fixed concentrations for $\delta E_t = 1.1e^2/\epsilon a$. The solid line joins the stable phases.

In order to study the stability of the ground states we introduce the chemical potential μ which controls the alkali content (x) in the system. The stable state as a function of μ is determined by the minimum of Gibbs potential per C_{60} defined as

$$\mathcal{G}_0 = \mathcal{H}_0 - \mu x \quad (14)$$

where the index 0 refers to zero temperature and \mathcal{H}_0 denotes the total energy per C_{60} . A simple numerical calculation gives the stable state as a function of μ and δE_t . The results are summarized in Fig. 5. This map shows that the alkali content increases with the chemical potential for a fixed δE_t . The energy relations are similar to those plotted in Fig. 4 if $\delta E_t > 1.0106e^2/\epsilon a$. There is a region of δE_t when the (0,0,0) state transforms directly to (1,1,1) for increasing μ as is suggested theoretically by Fleming *et al.* [6] If $\delta E_t < 0.1406e^2/\epsilon a$ then the (0,1,1) state is stable. This behavior is a consequence of the fact that δE_t does not give an energy contribution to the states (0,0,0) and (1,0,0) however, it shifts the energy of the states (0,1,1) and (1,1,1) by the same value.

We have evaluated the energies of several ordered states related to a different sublattice division of the tetrahedral sites. In order to determine the ground states of the systems both the octahedral and tetrahedral (FCC) lattices have been decomposed into four simple cubic lattices and the energies of all the possible ordered structures on the 12 sublattices have been calculated.

In comparison with previous results we obtained higher energies for all the states distinguishable from the former ones. This investigation confirms the above sublattice division thereby providing a framework for later analysis.

It is mentioned here that the ground state energies are independent of the screening mechanism. The role of this mechanism becomes important when studying the sublattice occupations as a function of temperature.

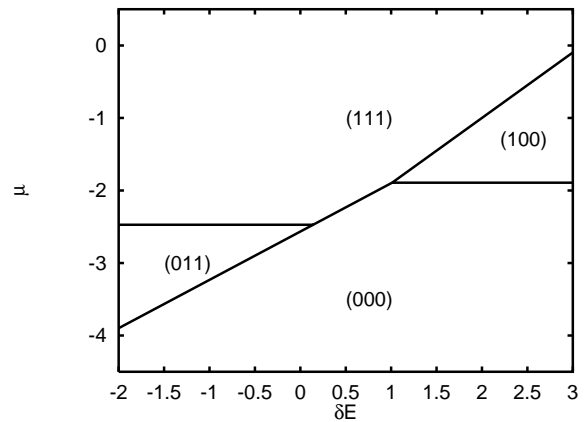


FIG. 5. Ground states of A_xC_{60} as a function of chemical potential μ and δE_t .

IV. MEAN-FIELD APPROXIMATION

In this section the thermodynamic properties of the lattice-gas model defined by the Hamiltonian (13) are investigated by using a three-sublattice mean-field approximation. It is assumed that the interstitial points are occupied by an alkali ion with the same probability σ_ν within the sublattice $\nu = 0, 1, 2$.

By means of the mean-field approximation the energy per C_{60} molecule may easily be expressed by the variables σ_ν as

$$\mathcal{H} = \sum_{\nu} \epsilon_{\nu} \sigma_{\nu} + \frac{1}{2} \sum_{\nu, \tau} J_{\nu\tau} \sigma_{\nu} \sigma_{\tau} \quad (15)$$

where the $J_{\nu\tau}$ coupling constants contain all the interactions between an alkali ion in sublattice ν and those ions residing in sublattice τ , i.e.,

$$J_{\nu\tau} = \sum_{j \in S_{\nu}} V_{ij}, \quad (i \in S_{\tau}). \quad (16)$$

where S_{ν} denotes the set of sites belonging to sublattice ν . The tensor of coupling constants is symmetric, that is, $J_{\nu\tau} = J_{\tau\nu}$. Furthermore, $J_{01} = J_{02}$ and $J_{11} = J_{22}$ because of the equivalence of the tetrahedral sublattices. Consequently, we have only four different coupling constants characteristic of the model in mean-field approximation. Their values may be determined by straightforward numerical calculation which gives

$$\begin{aligned} J_{00} &= -1.42879 \frac{e^2}{\epsilon a}, \\ J_{11} &= -1.60386 \frac{e^2}{\epsilon a}, \\ J_{01} &= -0.29000 \frac{e^2}{\epsilon a}, \\ J_{12} &= -0.86560 \frac{e^2}{\epsilon a} \end{aligned} \quad (17)$$

if $R/a = 0.312$. Notice that all the $J_{\nu\eta}$ are negative, i.e., the attractive forces rule over the short range repulsion (see Fig. 2).

Here it is worth mentioning that Eq. (16) permits some modification of pair interactions V_{ij} leaving the mean-field parameters (as well as the ground state energy) unchanged. For example, one can remove the interactions for large distances adding suitable corrections to the short range terms. In some sense the above screening mechanism may be considered as an example of such a process. This simplification may be very useful for Monte Carlo simulations. As a limit case, one can introduce a model characterized by the first four V_{ij} terms with a suitable choice of their strength.

It is evident that the mean-field Hamiltonian (15) reproduces the energies of the ordered states discussed above. However, the coupling constants $J_{\nu\eta}$ cannot be determined in the knowledge of the Madelung energies for all the ordered structure because this Hamiltonian contains more information, viz. it gives the potential energies for the empty sites too.

The thermodynamic properties of the system are determined by the minimization of Gibbs potential

$$\mathcal{G} = \mathcal{H} - TS - \mu \sum_{\nu} \sigma_{\nu} \quad (18)$$

with respect to σ_{ν} for fixed temperature T and chemical potential μ . In the above expression the configurational entropy per C_{60} is given as

$$\mathcal{S} = -k_B \sum_{\nu} [\sigma_{\nu} \log \sigma_{\nu} + (1 - \sigma_{\nu}) \log(1 - \sigma_{\nu})] \quad (19)$$

where k_B is the Boltzmann constant.

The results of the numerical calculations are summarized in temperature-composition ($T-x$) phase diagrams for different values of δE_t . The alkali concentration is related to sublattice occupations ($x = \sum \sigma_{\nu}$) determined directly by the numerical procedure.

In agreement with the ground state analysis, Fig. 6 illustrates that only the (0,0,0), (0,1,1) and (1,1,1) phases are stable at low temperatures for $\delta E_t = 0$. For intermediate compositions the system segregates into two phases as indicated in the figure. It is emphasized that in the high temperature phase the tetrahedral and octahedral sites are occupied with different probabilities. More precisely, the tetrahedral sites are preferred to the octahedral ones for $\delta E_t = 0$. For example, if the temperature is decreased for a fixed concentration $x = 2$ the present model suggests a continuous ordering process characteristic of the CaF_2 -type superionic conductors. [27]

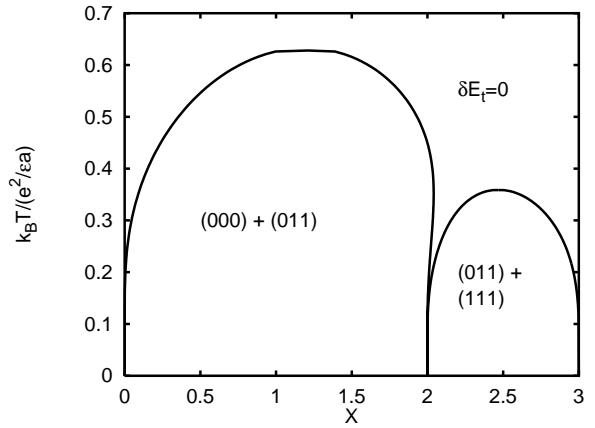


FIG. 6. Phase diagram for $\delta E_t = 0$ in mean-field approximation.

The (0,1,1) structure becomes unstable at $T = 0$ when $\delta E_t > 0.1406e^2/\epsilon a$. Fig. 7 shows a situation when the homogeneous (0,1,1) phase may be observed in the system but it decomposes into two states [(0,0,0)+(1,1,1)] at low temperatures. A eutectoid transition appears at $k_B T / (e^2 / \epsilon a) = 0.2442$ for $\delta E_t = 0.15e^2/\epsilon a$. To demonstrate this eutectoid transition the value of δE_t is chosen to be close to the threshold value of its stability at $T = 0$.

The decomposition of the high temperature phase into the phases (0,0,0) and (1,1,1) may be observed in a region of δE_t defined in Sec. III. A typical phase diagram that characterizes the phase separation at finite temperatures will be shown in the subsequent section.

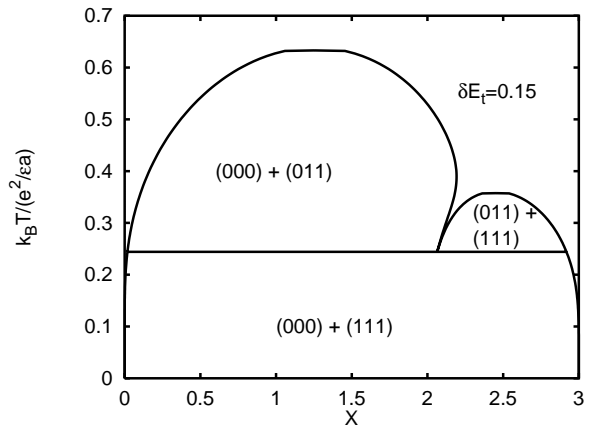


FIG. 7. Phase diagram in mean-field approximation for $\delta E_t = 0.15e^2/\epsilon a$ exhibits a eutectoid phase transition.

As mentioned above the energy of both the (0,1,1) and (1,1,1) phases increases with δE_t meanwhile the energy of the phases (0,0,0) and (1,0,0) remains unchanged, and the (1,0,0) phase appears in the phase diagrams for $\delta E_t > 1.0106e^2/\epsilon a$. More precisely, close to this stability threshold value one can observe a eutectoid transition (see Fig. 8) which is analogous to the situation discussed above. This phase diagram is similar to those suggested by Poiriet and Weaver [12] and Kuz-

many *et al.* [13] for the K_xC_{60} system for $x < 3$. With X-ray photoemission and Raman spectroscopy they observed a reversible transformation from KC_{60} to a mixed phase of C_{60} and K_3C_{60} at the eutectoid temperature ($T_{eut} = 150 \pm 10$ °C). For $\delta E_t = e^2/\varepsilon a$ the present approach predicts $k_B T_{eut} = 0.250e^2/\varepsilon a$.

A new type of phase diagram will be characteristic of the system when the (1,0,0) phase becomes stable at zero temperature. Instead of displaying now a typical plot, in Sec. V we compare the phase diagrams suggested by mean-field approximation and CVM for $\delta E_t = 1.1e^2/\varepsilon a$.

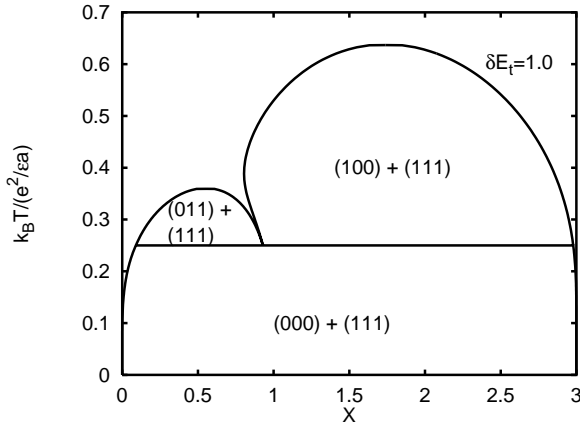


FIG. 8. Mean-field analysis of lattice-gas model suggests eutectoid phase transition for $\delta E_t = e^2/\varepsilon a$.

It is emphasized that in the above phase diagrams (including those plotted in Sec. V) both tetrahedral sublattices are occupied with the same probability implying the union of these sublattices. However, some modification of the model parameters results in the appearance of the (0,1,0) and (1,1,0) states. We have also evaluated some phase diagrams accepting the spherical shell model suggested by Rabe *et al.* [7] with a radius of the C_{60} molecule. In order to demonstrate the difference between these choices we display two phase diagrams corresponding to $R = 3.5$ Å. In the first example the (0,1,0) state is stable at $T = 0$ as illustrated in Fig. 9. The additional feature observable in this plot is the appearance of an order-disorder transition confined to tetrahedral sites for $x = 1$ meanwhile the octahedral sites are practically empty. This process is analogous to an “antiferromagnetic” to “paramagnetic” transition, in other words the (0,1,0) state transforms into (0,1/2,1/2) at a critical temperature ($k_B T_N = 0.555e^2/\varepsilon a$).

The mean-field analysis suggests a very interesting phase diagram for $\delta E_t = e^2/a$ (see Fig. 10). In this case, if the temperature for $x = 2$ is decreased the high temperature phase decomposes into two phases whose alkali concentrations are close to 1 and 3. At lower temperatures, however, the (1,1,0) phase becomes stable in comparison to the coexistence of states (1,0,0) and (1,1,1).

The richness of the predicted phase diagrams is surprising because we have varied only two parameters. Rigor-

ous analysis of all the possible diagrams as a function of R and δE_t , however, goes beyond the scope of the present paper.

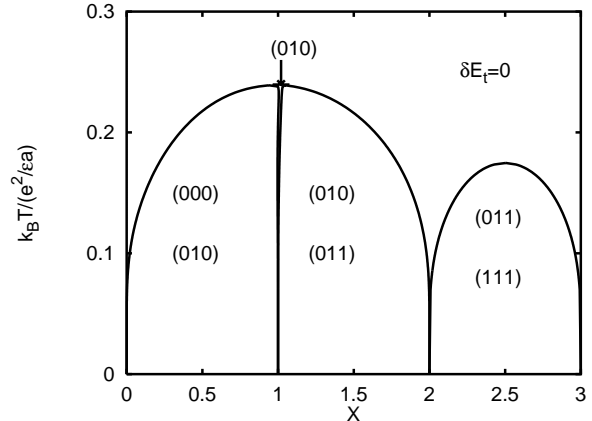


FIG. 9. Phase diagram for $\delta E_t = 0$ when the electronic energy of C_{60}^{x-} is approximated by a spherical shell model with radius 3.5 Å.

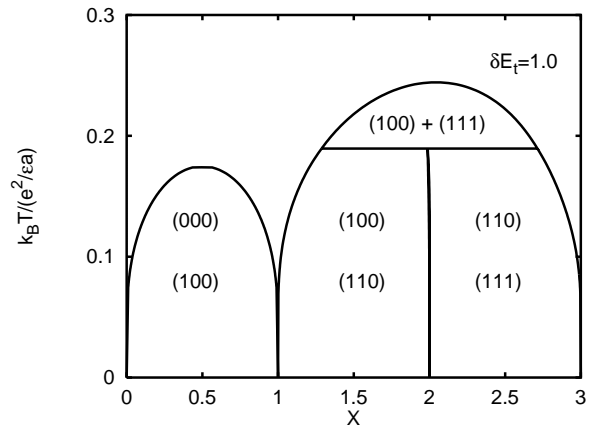


FIG. 10. Phase diagram for $\delta E_t = e^2/\varepsilon a$ and $R = 3.5$ Å.

V. CLUSTER-VARIATION METHOD

The cluster variation methods (CVM) are successfully used for deriving phase diagrams with sufficient accuracy. [28] Two basic difficulties emerge when adapting this technique to the present lattice-gas model. On the one hand, the interstitial sites form a non-Bravais lattice; on the other hand, instead of the usual first (and second) neighbor interaction(s) there are a lot of parameters V_{ij} characteristic of the interaction between sites i and j . Here we suggest the application of a simple version of CVM to increase the accuracy of the three-sublattice mean-field approximation.

First we introduce a set of variables $t(\eta_0, \eta_1, \eta_2)$ to denote the probability of a configuration (η_0, η_1, η_2) on three neighboring sites where η_ν refers to the occupation of the site belonging to sublattice ν . The position

of such a three-point cluster is indicated by a triangle in Fig. 3. The probability of a configuration on a part of this triangle may be easily expressed by the values of t . For example, the probabilities for pair configurations are given as

$$\begin{aligned} p_{01}(\eta_0, \eta_1) &= \sum_{\eta_2} t(\eta_0, \eta_1, \eta_2), \\ p_{02}(\eta_0, \eta_2) &= \sum_{\eta_1} t(\eta_0, \eta_1, \eta_2), \\ p_{12}(\eta_1, \eta_2) &= \sum_{\eta_0} t(\eta_0, \eta_1, \eta_2), \end{aligned} \quad (20)$$

and for single site configurations

$$\begin{aligned} s_0(\eta_0) &= \sum_{\eta_1, \eta_2} t(\eta_0, \eta_1, \eta_2), \\ s_1(\eta_1) &= \sum_{\eta_0, \eta_2} t(\eta_0, \eta_1, \eta_2), \\ s_2(\eta_2) &= \sum_{\eta_0, \eta_1} t(\eta_0, \eta_1, \eta_2) \end{aligned} \quad (21)$$

whose values are directly related to the sublattice occupations σ_ν introduced previously, namely $s_\nu(1) = \sigma_\nu$ and $s_\nu(0) = 1 - \sigma_\nu$.

The contribution of the first and second neighbor interactions to the system energy may be directly expressed by the variables $p_{\nu\tau}(1, 1)$ and only the remaining terms are approximated on the basis of mean-field theory. That is, now the energy per C_{60} molecule is given as

$$\begin{aligned} \mathcal{H}^{(CVM)} &= 4V(1)[p_{01}(1, 1) + p_{02}(1, 1)] + 6V(2)p_{12}(1, 1) \\ &+ \frac{1}{2} \sum_{\nu, \tau} J'_{\nu\tau} s_\nu(1) s_\tau(1) + \sum_{\nu} \epsilon_\nu s_\nu(1) \end{aligned} \quad (22)$$

where $V(1) = 0.27459e^2/\varepsilon a$ and $V(2) = -0.00386e^2/\varepsilon a$ denotes the interactions V_{ij} at the shortest and second shortest distances and $J'_{\nu\eta}$ is equivalent to $J_{\nu\eta}$ defined by Eq. (16) except the coupling constants should be reduced by the contributions of $V(1)$ and $V(2)$,

$$\begin{aligned} J'_{01} &= J_{01} - 4V(1), \\ J'_{12} &= J_{12} - 6V(2). \end{aligned} \quad (23)$$

Here we restrict ourselves to demonstrating how the entropy may be derived on the analogy of pair approximation developed by Bethe. [29] The non-Bravais lattice of interstitial sites may be built up by repeating periodically the triangle of an octahedral and two tetrahedral sites as prescribed by the primitive cell of FCC structure. This construction makes it clear that each triangle is surrounded by twelve triangles with the same orientation. According to the pair approximation the entropy is expressed by the probability of pair configurations. [29,30] In the present situation the probability of a configuration on a pair of triangles is approximated as a product

of $t(\eta_0, \eta_1, \eta_2)$ variables. The calculation leads to the following formula:

$$\begin{aligned} \mathcal{S}^{CVM} &= -6k_B \sum_{\eta_0, \eta_1, \eta_2} t(\eta_0, \eta_1, \eta_2) \log t(\eta_0, \eta_1, \eta_2) \\ &+ k_B \sum_{\nu < \tau} x_{\nu\eta} \sum_{\eta_\nu, \eta_\tau} p_{\nu\tau}(\eta_\nu, \eta_\tau) \log p_{01}(\eta_\nu, \eta_\tau) \\ &+ k_B \sum_{\nu} y_\nu \sum_{\eta_\nu} s_\nu(\eta_\nu) \log s_\nu(\eta_\nu) \end{aligned} \quad (24)$$

where $x_{01} = x_{02} = y_1 = y_2 = 2$ and $x_{12} = y_0 = 1$.

Substituting Eqs. (22) and (24) into (18) one obtains the Gibbs potential as a function of $t(\eta_0, \eta_1, \eta_2)$ variables. As is well known, \mathcal{G} reaches its minimum at the equilibrium values of these variables. In fact we have seven independent variables because the eighth configuration probability is determined by the condition of normalization. The numerical treatment is similar to those followed in mean-field approximation. The only difference, that instead of the three σ_ν variables now we have seven parameters to minimize the Gibbs potential with respect to them.

All the (mean-field) phase diagrams for $R/a = 0.312$ have been recalculated by using this technique. The comparisons between the results of mean-field approximation and CVM are demonstrated in Figs. 11 and 12. These phase diagrams are typical in the present model for the regions $0.1402 < \delta E_t/(e^2/a) < 1.0106$ and $\delta E_t > 1.0106e^2/a$ respectively. In both cases the CVM suggests lower transition temperatures in comparison with mean-field results. In general we can say that the difference is only a few percent for $R/a = 0.312$; however, it becomes larger for smaller R when the short range interactions are more repulsive.

In brief, this version of CVM confirms qualitatively the results of mean-field approximation and leaves its main conclusions unchanged.

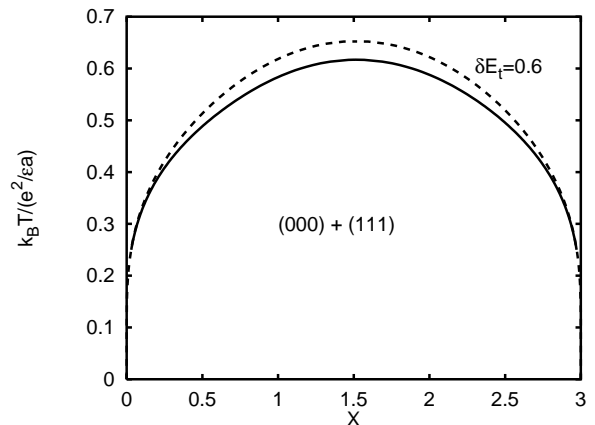


FIG. 11. Comparison of phase diagrams suggested by mean-field approximation (dashed line) and CVM (solid line) for $\delta E_t = 0.6e^2/\varepsilon a$.

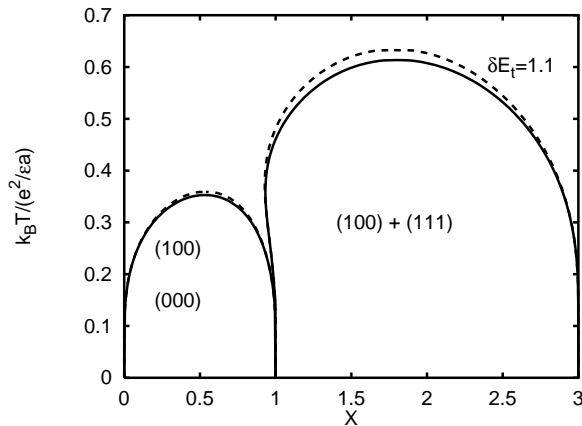


FIG. 12. Phase diagram for $\delta E_t = 1.1e^2/\epsilon a$ determined by mean-field approximation (dashed line) and CVM (solid line).

VI. SUMMARY AND CONCLUSIONS

We have developed a lattice-gas model for investigating the formation of different alkali intercalated fullerides with FCC structure. In this (Ising type) model the tetrahedral and octahedral interstitial sites of the cage lattice are empty or singly occupied by one type of alkali ion. It is assumed that the Coulomb interaction between two alkali ions is screened out by distributing their s electrons uniformly on their nearest neighbor C_{60} molecules. This plausible assumption results in a short range interaction which is very convenient for the lattice-gas formalism. For ordered structures this model reproduces the electrostatic energies found by previous authors. [6,7] At the same time this approach allows us to study the effect of electrostatic forces on the formation of different ordered and disordered structures at finite temperatures.

Besides the electrostatic energy the model takes into account the electronic energy of C_{60}^{x-} ions as well as the van der Waals interaction between an alkali ion and a C_{60} molecule. A series of UHF-MNDO calculations shows that the total energy of a charged C_{60} molecule has a term proportional to the square of its charge. This nonlinear contribution mediates an interaction between those alkali ions which transfer electrons to the same C_{60} molecule. This contribution is equivalent to the electrostatic energy of a charged spherical shell with radius R . The extra site energy (δE_t) characteristic of the van der Waals interaction at the smaller (tetrahedral) interstitial voids makes a distinction between the different types of alkali atoms. Without this term the tetrahedral sites are preferred in the system. In agreement with previous expectations [5,10] this energy contribution increases with the size of alkali atom and the octahedral sites are primarily occupied when δE_t exceeds a threshold value.

The thermodynamic properties of this model are investigated by using a three-sublattice mean-field approximation. The general features are illustrated via a series of phase diagrams. These diagrams draw a picture of

the effect of van der Waals interaction and the electronic energy of the C_{60}^{x-} ion on the ordering process. These results are confirmed qualitatively by CVM.

In the present approach the dielectric constant ϵ is considered as a parameter. A possible value ($\epsilon = 9$) may be estimated by fitting the experimental Raman shift in the A_6C_{60} fullerides. [32] Different values ($\epsilon \approx 4$) are suggested by Pederson and Quong [22] from the polarizability of C_{60} molecules. Desregarding the above uncertainty the maximum of the predicted ordering temperatures agree qualitatively with those expected on the basis of recent experiments. There are more reliable data on the phase separation temperature observed in the K_xC_{60} system. The present model can describe such type of phase diagrams (see Fig. 8) in a very narrow range of δE_t in agreement with the fact that this feature has not been observed for other fullerides. [33] Furthermore, applying pressure in order to contract the lattice the increasing δE_t will cause the sharp decrease of the eutectic temperature. Further increase of the pressure can even eliminate the phase separation and possibly an orthorhombic distortion of the cubic structure will appear typical of the A_1C_{60} systems at low temperature.

The ground state energy as a function of δE_t and the series of phase diagrams describe clearly that the A_2C_{60} composition can appear only for sufficiently low δE_t values corresponding to small atomic sizes as observed for $A=Li$ and Na .

The generalization of the present description for alkaline earth (or other) metals is straightforward. If the intercalated atoms have z valence electrons we should substitute a new energy unit, $(ze)^2/(\epsilon a)$ for $e^2/(\epsilon a)$ and find a suitable δE_t expressed in this unit. Due to the enhanced energy unit the A_2C_{60} composition can appear in a wider range of δE_t . At the same time the stronger Coulomb forces contract the lattice and modify the ratio R/a which can lead to some change in the phase diagrams.

The present approach is based on a simplified screening mechanism. This hypothesis may be very fruitful for investigating other intercalation compounds. The analysis of alkali intercalated fullerides with body-centered-cubic and -tetragonal structure is in progress.

ACKNOWLEDGMENTS

This research was supported in part by the Hungarian National Research Fund (OTKA) under Grants Nos. 2960 and F014378.

[1] A. F. Hebard, M. J. Rosseinsky, R. C. Haddon, D. W.

- Murphy, S. H. Glarum, T. T. M. Palstra, A. P. Ramirez, and A. R. Kortan, *Nature* **350**, 600 (1991).
- [2] M. J. Rosseinsky, A. P. Ramirez, S. H. Glarum, D. W. Murphy, R. C. Haddon, A. F. Hebard, T. T. M. Palstra, A. R. Kortan, S. M. Zaharak, A. V. Makhija, *Phys. Rev. Lett.* **66**, 2830 (1991).
- [3] K. Holczer, O. Klein, S.-M. Huang, R. B. Kaner, K.-J. Fu, R. L. Whetten, and F. Diederich, *Science* **252**, 1154 (1991).
- [4] J. E. Fischer and P. A. Heine, *J. Phys. Chem. Sol.* **54**, 1725 (1993).
- [5] J. H. Weaver and D. M. Poirier, *Solid State Physics* **48**, 1 (1994).
- [6] R. M. Fleming, M. J. Rosseinsky, A. P. Ramirez, D. W. Murphy, J. C. Tully, R. C. Haddon, T. Siegrist, R. Tycko, S. H. Glarum, P. Marsh, G. Dabbagh, S. M. Zahurak, A. V. Makhija, and C. Hampton, *Nature* **352**, 701 (1991).
- [7] K. M. Rabe, J. C. Phillips, and J. M. Vandenberg, *Phys. Rev. B* **47**, 13 067 (1993).
- [8] P. W. Stephens and L. Mihaly, *Phys. Rev. B* **45**, 543 (1992).
- [9] D. M. Poirier, T. R. Ohno, G. H. Kroll, P. J. Benning, F. Stepniak, J. H. Weaver, L. P. F. Chibante, and R. E. Smalley, *Phys. Rev. B* **47**, 9870 (1993).
- [10] M. J. Rosseinsky, D. W. Murphy, R. M. Fleming, R. Tycko, A. P. Ramirez, T. Siegrist, G. Dabbagh, and S. E. Barrett, *Nature* **356**, 416 (1992).
- [11] Q. Zhu, O. Zhou, N. Coustel, G. M. M. Vaughan, J. P. McCauley, Jr., W. J. Romanow, J. E. Fischer, A. B. Smith, *Science* **254**, 545 (1991).
- [12] D. M. Poirier and J. H. Weaver, *Phys. Rev. B* **47**, 10 959 (1993).
- [13] H. Kuzmany, M. Matus, T. Pichler, and J. Winter, in *Proceedings of NATO ARW Kreta, 1993*, NATO ASI-C series (in press); T. Pichler, R. Winkler, and H. Kuzmany, *Phys. Rev. B* **49**, 15 879 (1994).
- [14] O. Chauvet, G. Oszlányi, L. Forro, P. W. Stephens, M. Tegze, G. Faigel, and A. Jánossy, *Phys. Rev. Lett.* **72**, 2721 (1994).
- [15] S. Saito and A. Oshiyama, *Phys. Rev. B* **44**, 11 536 (1991).
- [16] S. Satpathy, V. P. Antropov, O. K. Andersen, O. Jepsen, O. Gunnarsson, A. I. Liechtenstein, *Phys. Rev. B* **46**, 1773 (1992).
- [17] J. Hubbard and J. B. Torrance, *Phys. Rev. Lett.* **47**, 1750 (1981).
- [18] R. Magri, S.-H. Wei, and A. Zunger, *Phys. Rev. B* **42**, 11 388 (1990).
- [19] Z. W. Lu, S.-H. Wei, A. Zunger, S. Frota-Pessoa, and L. G. Ferreira, *Phys. Rev. B* **44**, 512 (1991).
- [20] M. van Schilfgaarde, A.-B. Chen, and A. Sher, *Phys. Rev. Lett.* **57**, 1149 (1986).
- [21] R. M. Metzger, *Mol. Cryst. Liq. Cryst.* **85**, 97 (1982).
- [22] M. R. Pederson, A. A. Quong, *Phys. Rev. B* **46**, 13584 (1992).
- [23] M. J. S. Dewar and W. Thiel, *J. Am. Chem. Soc.* **99**, 4899 (1977).
- [24] V. de Coulon, J.L. Martins, F. Reuse, *Phys. Rev. B* **45**, 13671 (1992).
- [25] K. Yamaguchi, S. Hayasi, M. Okumara, M. Nakano, W. Mori, *Chem. Phys. Lett.* **226**, 372, (1994).
- [26] C. J. F. Bottcher, *Theory of Electric Polarization*, (Elsevier, Amsterdam, 1952)
- [27] See S. Chandra, *Superionic Solids* (North-Holland, Amsterdam, 1981).
- [28] For a recent review see D. de Fontaine, in *Alloy Phase Stability*, Vol. 163 of NATO ASI Series E Applied Sciences, Edited by G. M. Stocks and A. Gonis (Kluwer, Dordrecht, 1989).
- [29] H. A. Bethe, *Proc. Roy. Soc. (London)* **A150**, 552 (1935).
- [30] S. K. Aggarwal and T. Tanaka, *Phys. Rev. B* **16**, 3963 (1977).
- [31] J. H. Kim, A. Petric, P. K. Ummat, and W. R. Datars, *J. Phys. C* **6**, 5387 (1994).
- [32] S. Sanguinetti, G. Benedek, *Phys. Rev. B* **50**, 15439, (1994)
- [33] D. Koller, M.C. Martin, L. Mihály, *Mol. Cryst. Liq. Cryst.* **256**,275 (1994).